ACS OMEGA

Open Access

http://pubs.acs.org/journal/acsodf

Article

Tack Properties of Nanostructured Epoxy−Amine Resins on Plasma-Treated Glass Substrates

Olivier Tramis, Nicolas Merlinge, Bouchra Hassoune-Rhabbour, Marina Fazzini, and Valérie Nassiet*

Cite This: *ACS Omega* 2023, 8, 37842−37851

Read Online

ACCESS | Metrics & More | Article Recommendations | Supporting Information

ABSTRACT: A probe tack test, coupled with in situ imaging, was used to evaluate the influence of an air plasma treatment on glass substrates on the fracture energy of nanostructured epoxy−amine resins. Nanostructuration was achieved by the addition of thermoplastic triblock copolymers. The influence of the surface treatment was assessed by splitting the fracture energy (tack energy) into three main contributions (cavitation, viscous flow, and stretch). We showed that before gelation, the interfacial strength depended on the nature of the copolymers and on their interaction with grafted functions (R−COOH and R−C═O) by air plasma treatment. The latter also influenced the cohesion of the resins, impacting the copolymers' phase separation and, as a consequence, conversion rate. The tack test, coupled with rheology and thermal (differential scanning calorimetry) measurements, was relevant to explain how the balance of interactions contributed to the fracture energy up to the gel point.

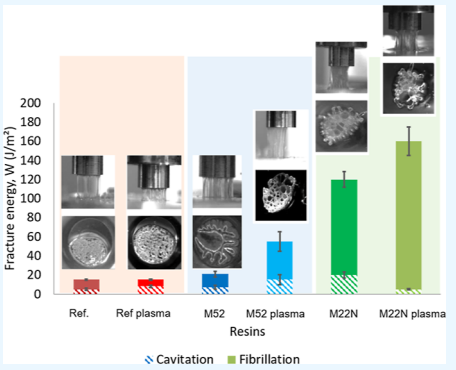

1. INTRODUCTION

Glass is a material that is widely used in numerous applications. Due to its intrinsic brittleness, adhesive bonding is the premium choice when joining glass. The surface of the glass must be cleaned to ensure a good level of adhesion with an adhesive. Plasma treatments are efficient and versatile methods to clean glass, and depending on the type of plasma used, various surface properties of the glass may be modified. Abenojar et al. measured an increase of surface valley, leading to an increase of surface roughness when treating the glass by an atmospheric pressure plasma torch.[1] Surface modification resulted from an etching effect, mostly due to the high power used (21 kV). Terpilowski and Rymuszka, however, noted smoothening of the glass by a low-pressure gas (nitrogen, oxygen, air, and argon) plasma. They also noted that the plasma treatment grafted polar oxygen-based functions for all the aforementioned plasmas.[2] The quantity of polar groups grafted depended on the plasma used. For instance, air and oxygen plasmas were reported to graft carboxyl (═C−OH), ketone (═O), and hydroxyl (C−OH) groups. Dry air plasma (air with a relative humidity of 4%) provoked breakage of the O−OH bonds of already adsorbed water on the surface in hydroxyl (C−OH) and ketone (C═O) groups.[3]

Tack tests on epoxy resins are used to assess the stickiness of prepregs.[4] This peculiar property is needed for reliably positioning the prepreg during manufacturing, as well as to prevent sliding during lay-up of a laminate.[5,6] In all cases (bonding glass, prepreg manufacture, etc...), the nanostructuration of the epoxy resins and the influence of the substrates' surface treatment are key parameters directly influencing the stickiness.[6] In a previous report,[7] we used a probe tack test on a glass coated with epoxy−amine resins nanostructured by thermoplastic triblock copolymers. By using this test, we were able to discriminate the influence of the copolymers on the interfacial strength, on the one hand, and cohesion, on the other hand. Briefly, copolymers enhanced the cohesiveness of the resin, while their interactions with the surface were inferred to enhance the interfacial strength at the glass/resin interface. Therefore, we were able, with the tack test, to highlight the balance between the interfacial strength governing the cavitation, linked to the reversible Dupré energy, caused by short-range forces (VdW, hydrogen bonding, etc.) and the energy dissipated during the test, including interfacial dissipation and from the resins' cohesiveness.[8]

In the present study, we first attempt to understand the interactions' balance within the resins (epoxy, amine, and copolymers) and mixtures (epoxy and copolymers) through low-frequency rheology. We then use the probe tack test to investigate how a modification of the surface properties by atmospheric plasma impacts, on the one hand, both the interfacial strength and cohesion of the nanostructured resins and, on the other hand, the interactions' balance of the components.

Received: April 25, 2023
Accepted: September 20, 2023
Published: October 4, 2023

2. EXPERIMENTAL SECTION

2.1. Preparation of the Resins. The resin referred to as reference was obtained by mixing diglycidyl ether bisphenol A (DGEBA) (DER332, Sigma-Aldrich) with 3,4-methylenedioxy-*N*-ethylamphetamine (MDEA, obtained from Lonzacure) under vigorous stirring at 160 °C until a homogeneous, transparent mixture was obtained. Subsequent degassing under vacuum (20 min under 1 bar depression) was needed to remove trapped air bubbles.

Nanostructured resins were obtained by adding amphiphilic thermoplastic triblock copolymers (Nanostrength, Arkema). The M52 copolymers were composed of PMMA-*b*-PBA-*b*-PMMA (PMMA: polymethyl methacrylate and PBA: polybutyl acrylate), while the M22N copolymers were composed of PMMA-(co-DMA)-*b*-PBA-*b*-PMMA-(co-DMA), where dimethylacrylamide (DMA) was grafted onto the PMMA blocks to improve the miscibility of M22N within DGEBA.[9]

The reference was obtained by incorporating MDEA at 160 °C into DGEBA, until a homogeneous, transparent mixture was obtained.

The nanostructured resins were obtained by adding 10 wt % copolymers (either M52 or M22N) to DGEBA under vigorous stirring at 160 °C until complete incorporation. Then, MDEA was added at 160 °C until a homogeneous, transparent mixture was obtained. Degassing was conducted under 1 bar depression at 120 °C for 20 min. The resin made with M52 (M22N) was referred to as M52 resin (M22N resin).

In Section 3.2, only a mixture of DGEBA and copolymers (mixed as 10 wt %) was used. DGEBA and 10 wt % of copolymer mixtures were referred to as DER + M52 mixture or DGEBA + M22N mixture, depending on the copolymer used.

It is important to note that the DGEBA−copolymers-10% mixture is much more viscous than the resin itself, i.e., the addition of MDEA decreases the viscosity.

2.2. Preparation of the Substrates. Inorganic glass substrates (microslides plain, Corning, with a rough composition of 70% SiO_2, 15% Na_2O, 10% CaO_2, and 5% metal oxides) were cut into rectangular dimensions ($55 \times 45 \times 1$ mm^3). Two surface preparations were used. The first treatment is a simple cleaning of the glass plates, by immersion and ultrasonication in acetone for 10 min, as the first surface preparation, referred to as "degreasing". For the second surface treatment, cleaning as for the degreased substrates was performed, followed by an air plasma treatment performed on an industrial device (the plasma generator Openair FG5001 with the rotary nozzle RD1004, Plasmatreat, France). Optimization of the parameters gave the following: the nozzle was positioned 2 cm above the substrate, the power was set at 1 kV, the velocity was set at 2.2 mm/s, and the nozzle passed four times over the sample at the set velocity. This surface preparation is referred to as "plasma". Air plasma treatment modified the glass surface energy by increasing both dispersive and polar components, the former being more increased than the latter (Table 1). The increase of the dispersive component may be attributed to an increase in the concentration of bridged oxygen in Si−O groups on the outer surface, as reported for similar inorganic glasses.[1,10] The polar contribution increase may be mainly attributed to an increase of grafted hydroxyl groups,[2,3] even though grafted carboxyl and ketones may also contribute.

2.3. Preparation of the Samples for Probe Tack Tests. A 300 μm-thick PTFE mask was deposited onto the degreased surface to delimit the surface. The subsequent plasma treatment was always performed after positioning the mask to avoid any mishandling and contamination. Resins were spread throughout the mask. Then, the samples were degassed under 1 bar depression for 30 min at ambient temperature, in order to remove as many preformed air bubbles as possible. The samples were put in an oven at 120 °C for 130, 110, and 130 min for the reference, M52 resin, and M22N resin, respectively. The samples were then cooled quickly to room temperature and then tested right away.

Table 1. Free Surface Energy of Glass before (AU) and after Plasma Treatment (P4P), Measured by the Owens−Wendt Method[11]

surface treatment	degreasing	plasma
free surface energy (J/m^2)	52.2 ± 1.6	74.7 ± 0.4
polar component	30.6 ± 1	35.7 ± 0.3
dispersive component	21.6 ± 0.7	38 ± 0.5

2.4. Preparation of the Samples for Rheology. *2.4.1. Low-Frequency Rheology.* A commercial strain-controlled rheometer (Rheometric Dynamic Analyzer ARES, Rheometric Scientific Inc.) was used to obtain rheological data. A plate−plate geometry was used, with 50 mm diameter plates. The gap was set at 500 μm. 80% of strain was applied during the frequency sweep from 10 to 10^{-2} rad/s at room temperature. Preliminary strain sweeps were carried out to ensure that all of the experiments stayed within the linear viscoelastic domain.

2.4.2. Determination of the Tack Interval. The time the samples were left in the oven corresponded to the curing time which gives the maximum of tack energy for degreased substrates, determined during our previous study.[7] Briefly, the resins were placed between parallel plates (diameter 25 mm) and cured for some time at 120 °C. The first curing time was the time for which the moduli G' and G'' crossed (the crossover). After this time, the plates were quickly cooled down. Once at room temperature, we measured the complex viscosity by performing a frequency sweep. Winter[12] showed that, at low frequency during a frequency sweep, the curvature of the complex viscosity was linked to the gel state of the system. Systems behaving as solids were found to have a curvature of −1, while systems behaving as liquids had a curvature of 0. At the crossover, the resins showed solid-like behavior, characterized by a curvature −1 in a complex viscosity/frequency diagram (Supporting Information Figure S1). 2 hours before the crossover, the resins showed a liquid-like behavior, characterized by a curvature 0. Therefore, we defined the tack interval as the curing times comprised between those which gave the last liquid-like behavior and the first solid-like behavior, at room temperature (Supporting Information Figure S1). It shall be noted that the tack interval is thus 40 min long for both the reference and M52 resin, while it is 60 min long for the M22N resin. We discuss possible reasons in Section 3.2.

We then assumed that resins on the glass substrates behaved as determined by the frequency sweeps. Therefore, some resin was sampled from the glass substrate to evaluate the conversion rate, calculated from eq 1 as follows

$$\alpha = 1 - \frac{\Delta H_{\text{residual}}}{\Delta H_{\text{max}}} \quad (1)$$

https://doi.org/10.1021/acsomega.3c02836
ACS Omega 2023, 8, 37842−37851

Anisothermal differential scanning calorimetry runs measured the residual heat, $\Delta H_{residual}$, at 3 °C/min, of the sampled resin. The maximal enthalpy for this ramp was known as ΔH_{max} for each resin. Following the conversion rate within the tack interval allows us to make assumptions about the interaction balance of the component. For instance, thermosetting resins are known to exhibit autocatalytic cross-linking, with their associated conversion rate following a sigmoidal law.[13] Thus, any changes provoked by the surface treatment may affect the conversion rate kinetics.

Moreover, Zosel[14] determined, for model PDMS, that the maximum in tack energy was found between the gel point (defined by the congruence of the moduli as defined by Winter[15]) and a solid-like behavior (defined as the storage modulus independent of the angular frequency), where the polymer's soluble fraction is still large. Therefore, the value of the conversion at which the maximum tack energy is measured is the value at which the resins behave as gels. Table 2 shows the data for the conversion rate as a function of the surface treatment at the curing time that gave the maximum tack energy.

Table 2. Curing Time Gives the Maximum Tack Energy at 120 °C and Associated Conversion Rate for the Resins[a]

resin	curing time (minutes)	conversion rate—degreased	conversion rate—plasma
reference	140	0.51	0.48
M52	110	0.42	0.32
M22N	130	0.31	0.36

[a]Uncertainties are ca. 4 min on the curing times and ca. 0.04 on the conversion rates.

Our data are in agreement with Zosel's assumptions, as the maximum of the tack energy was systematically found just before the first solid-like behavior (Table 2 and Supporting Information Figure S1), at respectively, 140, 110, and 130 min for the reference, M52, and M22N resins.

It also appears that regardless of the surface treatment, the maximum of the tack energy did not depend on the curing time for a given resin (Supporting Information Figures S5 and S6). However, the conversion rate did depend on the surface treatment. We discuss it further in Section 3.2.

2.4.3. Probe Tack Tests. Probe tack tests were dimensioned on a commercial stress-controlled rheometer (MCR302, Anton Paar), following our previous work.[7] A smooth probe, machined from a steel tube to a final diameter of 6 mm and polished to a mirrorlike finish, with a roughness of ca. 33 nm, was mounted on the mobile arm of the rheometer. The probe was moved down at 10 μm/s until contact with the resin. Upon contact, a constant force of 5N was applied for a dwelling time of 10 s. After this time, the probe was removed at a constant velocity of 100 μm/s. The rheometer recorded displacement−normal force curves, which were converted to stress−strain curves with the following relationships (eq 2)

$$\sigma = \frac{\text{Normal force}}{\text{Contact area}}; \qquad \varepsilon = \frac{\text{Displacement}}{\text{Initial thickness}} \tag{2}$$

3. RESULTS AND DISCUSSION

3.1. Low-Frequency Rheology. We tested through low-frequency rheology both DER−copolymer mixtures and the resins (epoxy, amines, and copolymers). The aim was to unveil any structural differences.

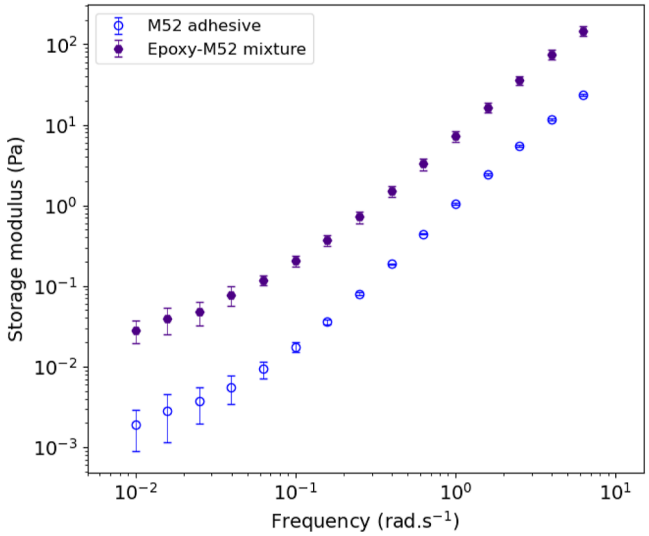

Figure 1. Storage modulus as a function of the frequency in a low-frequency sweep of the epoxy−M52 mixture and the M52 resin.

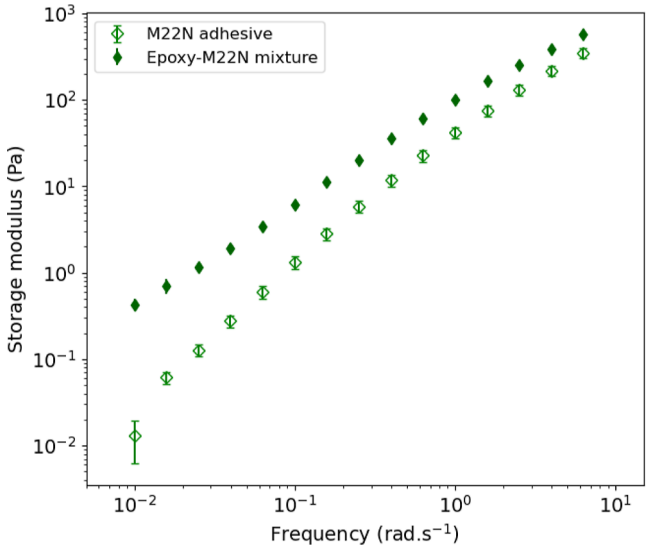

Figure 2. Storage modulus as a function of the frequency in a low-frequency sweep response of the epoxy−M22N mixture and the M22N resin.

Figure 1 shows the storage modulus associated with the DER−M52 mixture. A major feature is the apparition of a plateau from 0.1 rad/s, regardless of the presence of amines. The frequency at which the plateau appears indicates the relaxation time of clusters formed by the copolymers. Higher frequency means lower relaxation time, thus larger clusters.[16] The presence of the amines, the least viscous component in the resin, decreases only the resin's viscosity. It does not influence the plateau's apparition, hinting that copolymer−amine interactions are much weaker than epoxy−copolymers interactions.

In Figure 2, it can be seen that there is no plateau for either the DER−M22N mixture or the M22N resin. The absence of plateau indicates that the M22N copolymers form clusters much smaller than the M52 copolymers because of an expected increase in solubility. Interestingly, the slope of the

https://doi.org/10.1021/acsomega.3c02836
ACS Omega 2023, 8, 37842−37851

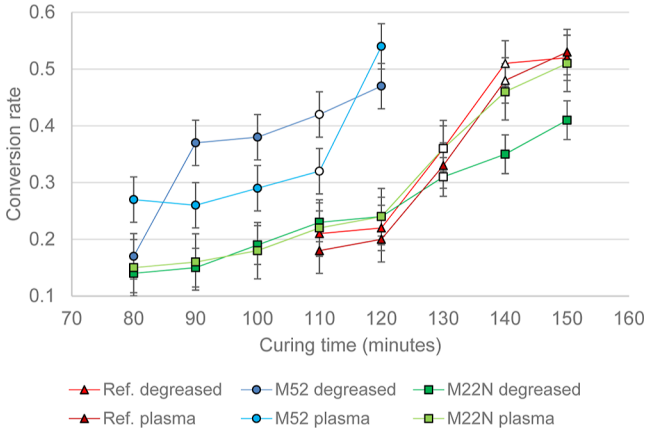

Figure 3. Conversion rate of the resins as a function of the curing time within the tack interval. Open keys represent the conversion at which the maximum of the tack energy was measured.

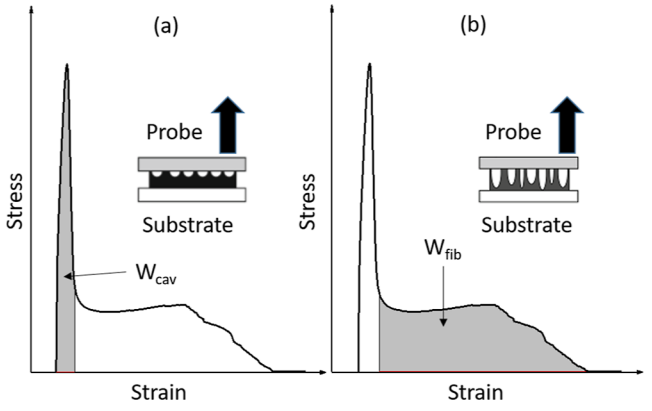

Figure 4. Representation of a tack test: (a) cavitation and associated tack energy (W_{cav}) and (b) fibrillation and associated tack energy (W_{fib}).

highest decade (from 10 to 1 rad s^{-1}) of the resin is the same as that of the lowest decade (from 0.01 to 0.1 rad s^{-1}) of the mixture, both being equal to 1.2. It is therefore difficult to assess with certainty if the amines really disrupt the epoxy–copolymer interactions or if the amines have a simple dilution effect, leading to a shift of the relaxation time spectrum, thus a shift in the frequency responses.

3.2. Influence of the Plasma Treatment on the Conversion Rate of the Resins. We investigated the degree of curing of the resins with respect to surface treatment. Before dealing with the influence of the plasma treatment, we shall give some insight into the conversion rate of the resins with respect to their copolymers' content.

The conversion rates as a function of the curing time are given in Figure 3, with Supporting Information Figures S2–S4 giving the same data for each resin separately.

The conversion rate associated with the reference exhibits a sigmoidal shape that is the common shape for an autocatalytic reaction, as expected from thermosetting resins.

The conversion rate associated with M52 also has a sigmoidal shape but shifted toward shorter curing times, as if the autocatalytic reaction took place earlier than for the reference. We remind that M52 contains triblock copolymers made of PBuA and PMMA. In the case of PMMA/epoxy–amine ternary blends, it has been reported by several groups that the cross-linking reaction can be either accelerated[13,17,18] or delayed[13,19] depending on the interactions between the components. In all cases, phase separation of PMMA occurs, and it increases as the curing reaction goes on up to gelation.

Acceleration of the curing reaction was attributed to phase separation of the initially miscible DGEBA/PMMA mixture, PMMA entrapping some DGEBA in PMMA-rich phases, breaking the stoichiometric balance toward an excess of hardener.

Delayed curing comes from a dilution effect of PMMA, where it may lower the viscosity of the epoxy–amine mixture's viscosity. Moreover, in the case in which PMMA is immiscible with the hardener, PMMA may rather self-associate than to interact with the hardener, increasing the curing delay.

In our case, we may suppose that phase separation takes place in the M52 resin since the cross-linking's acceleration happens before the M52 resin starts to behave as a gel. Moreover, those observations may hint that the M52 copolymers self-organize as rather large structure during the curing, as reported for similar copolymers in similar epoxy–amine systems.[20]

Oppositely, the conversion rate associated with the M22N resin does not exhibit a sigmoidal shape, at least on the times studied. The M22N resin contains PMMA on which are grafted DMA groups, with the aim to increase the PMMA miscibility with the epoxy resin and hence the copolymers' mobility. This explains that the M22N resin behaved as a gel after a curing time (130 min) much closer to that of the reference (140 min) than the M52 resin (110 min). This may point toward the occurrence of a "stronger" competition between the epoxy–copolymers and the epoxy–amine interactions, balancing the PMMA phase separation in the absence of DMA, as hinted for the M52 resin.

It appears clearly that the plasma treatment does not modify the conversion rate for the reference despite a slight decrease on average. The reference was found to behave as a gel (i.e.,

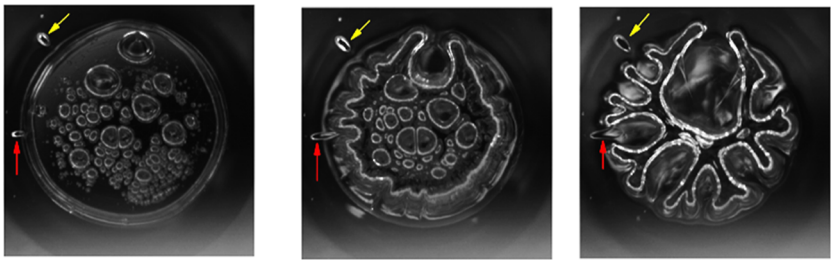

Figure 5. Illustration of a viscous flow taking place during a tack test. M22N resin, nontreated substrates, bottom view. The red and yellow arrows indicate bubbles stretched toward the center of the probe by the viscous flow. Images are 8.5 × 8.5 mm^2.

https://doi.org/10.1021/acsomega.3c02836
ACS Omega 2023, 8, 37842–37851

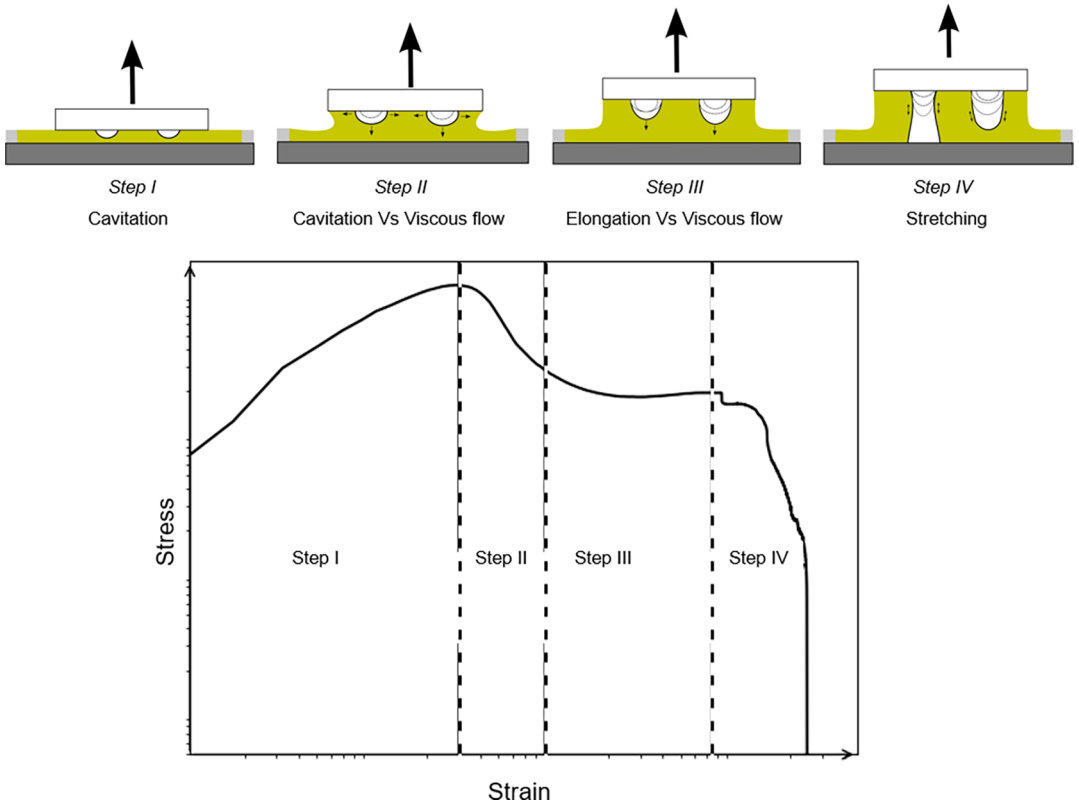

Figure 6. Double logarithmic scale representation of a probe tack test and description of the transient phenomenon occurring during a probe tack test for partially cured epoxy resins.

the first −1 slope on Supporting Information Figure S1) after 140 min of curing, just at the end of the sigmoid, with values independent of the surface treatment. While it is known that amine reacts with ketones through a condensation reaction,[21,22] it has been shown that amine−amine interactions are stronger than the amine−ketone ones in epoxy−amine resins.[13] Our results indicate that, in any case, the surface-grafted functional groups, and especially the carboxyl groups, containing a ketone, do not react enough with the amine to have a significant impact on the measured conversion rate.

The plasma treatment affected the conversion rate when copolymers were present. It shifted the conversion rate toward longer curing time for the M52 resin, as the sigmoidal shape occurs much later than on nontreated substrates. Inversely, the conversion rate for the M22N resin increased just before the gel-like behavior (gel as defined by Winter[11]). Thus, the plasma treatment changed the balance of interactions.

We suppose for the M52 resin that the ketone−amine condensation reaction is not significant enough to be seen. However, PMMA contains a ketone function, which may also interact with the grafted ketones, disrupting PMMA's phase separation. This also explains that the M52 resin was found to behave as a gel (gel as defined by Winter[11]) after the same curing time but for a weaker conversion rate on the plasma-treated substrates.

We suppose for the M22N resin that the plasma-grafted ketones may decrease the PMMA miscibility since DMA grafted on PMMA also contains a ketone function, adding more ketone−ketone interactions to the balance. A decrease in miscibility due to more ketone−ketone interactions from both PMMA and grafted DMA would lead to a higher phase separation, shifting the stoichiometry toward an excess of hardener. This structural change may be supported by the fact that the acceleration of the curing kinetics occurs before the resin reaches a gel-like behavior.[13] Indeed, the gel-like behavior was measured after 130 min of curing, just before the conversion rate's acceleration.

3.3. Probe Tack Tests. The probe tack is an ubiquitous test that is able to discriminate finely the cohesion and interfacial strength contribution of an adhesive.[7] In a stress−strain diagram, as depicted in Figure 4, the area under the curve, known as the tack energy, W (equivalent to a fracture energy, expressed in J/m^2), depends on two main contributions, namely, cavitation (Figure 4a) and fibrillation[23] (Figure 4b).

While this description is sufficient for thermoplastic polymers, as extensively demonstrated for pressure-sensitive adhesives (PSA), it may not be sufficient to describe thermosetting resins. Indeed, as reported in our previous study,[7] the tack of thermosetting polymers is accompanied by a viscous flow. To highlight its existence, we manually placed bubbles as tracers slightly outside the contact zone. They appear to be stretched toward the probe's center (Figure 5), highlighting the flow's occurrence. We only added those tracers for the sake of demonstrating the existence of the viscous flow since the degassing step removed preformed air bubbles.

Viscous Poiseuille flows in tack experiments have been reported for silicon oils, for which it is the main dissipative mechanism in combination with cavitation,[24] as the oils used are not able to form fibrils. The flow always follows cavitation, and the two contributions could be distinctly seen with a probe tack test.[24] In the case of thermosetting resins, the viscous flow comes from uncured monomers. This flow not only opposes cavitation but also opposes fibrillation, both competition

https://doi.org/10.1021/acsomega.3c02836
ACS Omega 2023, 8, 37842−37851

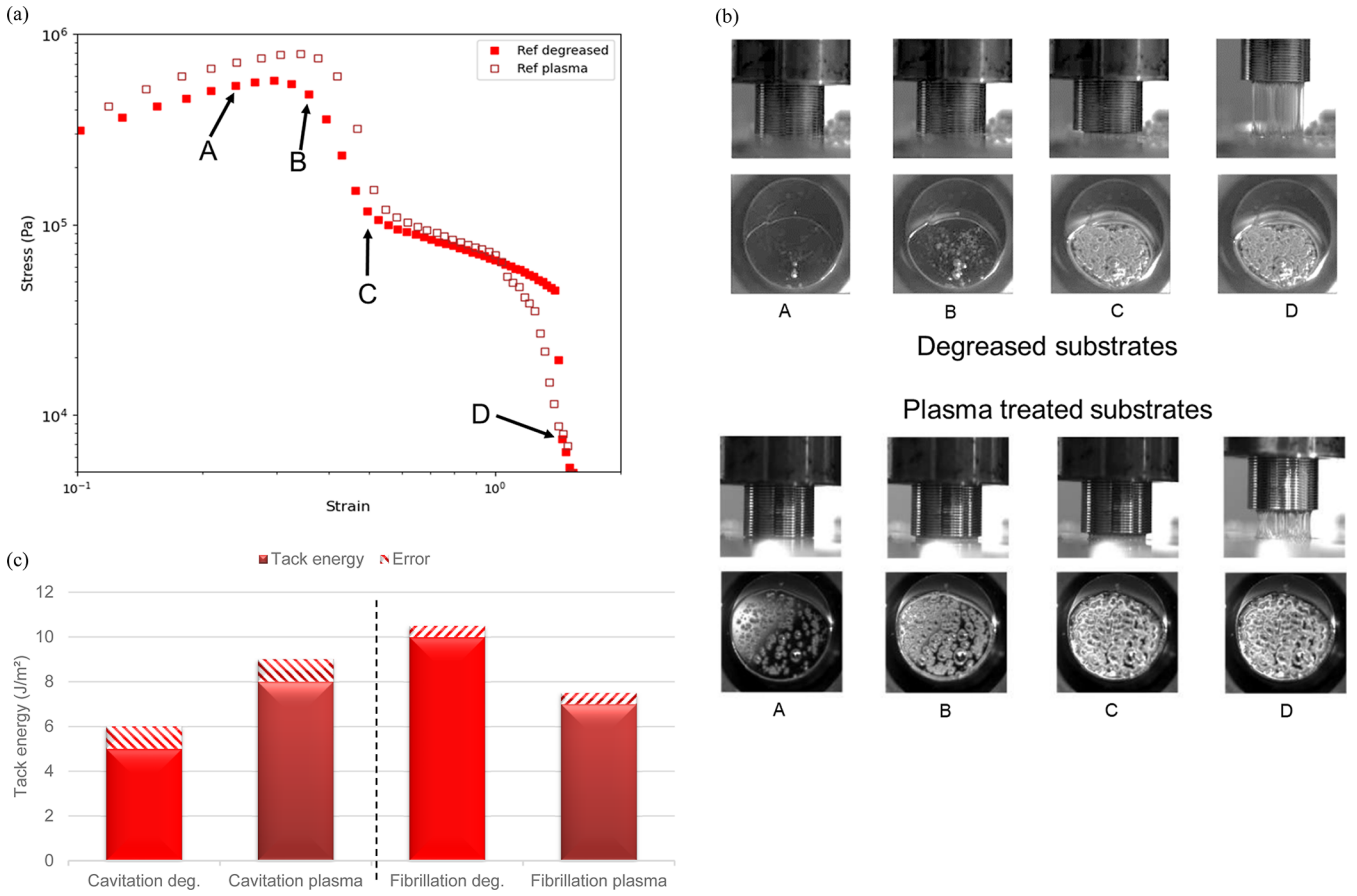

Figure 7. Tack data analysis of the reference resin. (a) Trend of tack curves for the reference, for both degreased (closed symbols) and plasma (open symbols) surface treatments, after an isothermal curing of 140 min at 120 °C. (b) Sampled images from a tack test to illustrate the dissipative phenomenon: A: cavitation; B: fibrillation (flow); and C and D: fibrillation (stretching). Images are 8.5 × 8.5 mm^2. (c) Tack energy on the degreased substrates, with details of contributions.

providing a new dissipative mechanism to take into account for thermosetting resins. In the former situation, the viscous flow tries to "swallow" the cavities, preventing their—mainly lateral—expansion. In the latter case, the viscous flow prevents fibrillation by extending the macromolecular orientation time span and delaying the actual stretching of the oriented macromolecules.

Therefore, partially cross-linked thermosetting resins, before their gel point, have the feature to display both viscous flow as silicon oils as well as fibrillation as for PSAs. This characteristic makes thermosetting resins stand out, as it is necessary to now include a contribution to W from the viscous flow. We propose to split the fracture energy in four parts (Figure 6): (I) cavitation, i.e., the three-dimensional growth of the cavities during the early stage of the tack test. The steeper the slope, the stronger the cavitation; (II) a transition step, marking the beginning of the viscous flow. During this step, cavities formed in step (I) may continue their triaxial growth. The steeper the slope, the less the resin is able to flow. Moreover, the longer the "plateau", the more the resin is able to flow;[20] (III) a step of competition between vertical, uniaxial stretching of cavities and the viscous flow. The smoother the slope, the more the resin flows; (IV) stretching, where all the macromolecules are oriented in the direction of the probe's lift and begin to disentangle. Most of the energy dissipated during a tack test comes from this step, especially if the cavities are stable enough not to be swallowed by the viscous flow and if the polymer is able to be stretched extensively, i.e., fibrillation. A horizontal slope (i.e., a plateau) depicts a stable yet energy-consuming, competition. Inversely, a nonhorizontal slope may indicate that the viscous flow dominates fibrillation. Strain hardening may occur, meaning that disentangled macromolecules are now stretched and can be seen by a stress increasing at the end of the plateau. Step (I) corresponds to a cavitation energy, step (II) to a viscous flow energy, and steps (III) and (IV) to a stretch energy, with the fibrillation contribution being at least formed by steps (III) and (IV) but being possibly formed of both the flow energy (step (II)) and the stretch energy. As a consequence, tack curves were plotted on a double log scale in order to expand graphically the transient phenomenon occurring throughout the test.

The measure of the tack energy included four measurement points by sample, on three different samples, one resin totalizing 12 measurements.

The method to determine the range for which the tack energy was measurable and its actual measure on degreased substrates was reported earlier.[7] For all resins and both treatments, the tack energy passed through a maximum.[7] The isothermal cross-linking time at which the maximum of tack was recorded for both treatments is shown in Table 2. As explained in the section about the samples' preparation, the plasma treatment did not influence the isothermal cross-linking time that gave the maximum tack but changed the actual values of the tack energy, as will be discussed below. The influence of

https://doi.org/10.1021/acsomega.3c02836
ACS Omega 2023, 8, 37842−37851

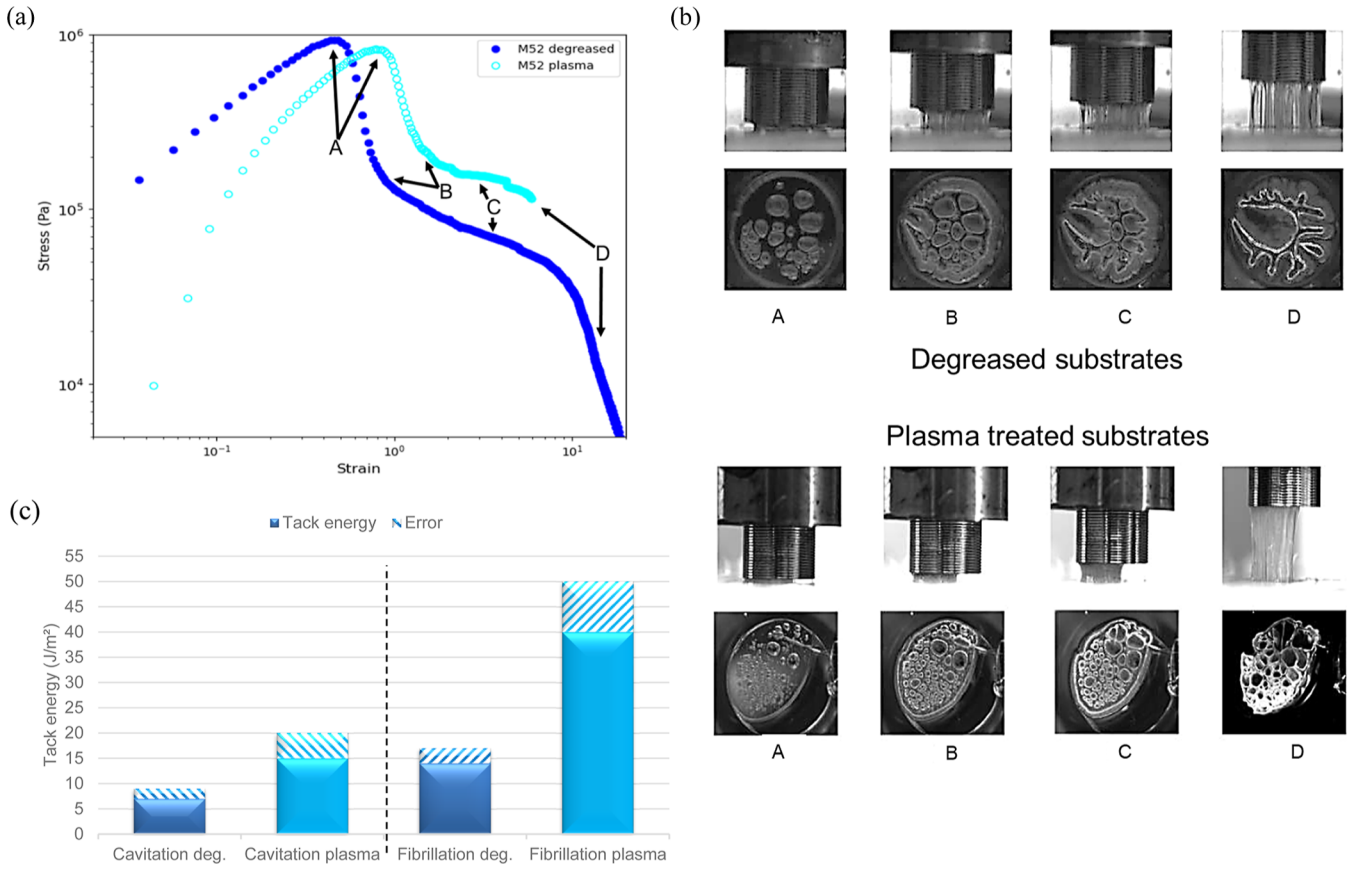

Figure 8. Tack data analysis of the M52 resin. (a) Trend of tack curves for the M52 resin, for both degreased (closed symbols) and plasma (open symbols) surface treatments, after an isothermal curing of 110 min at 120°. (b) Sampled images from a tack test to illustrate the four zones of Figure 5. A: cavitation; B: fibrillation (flow); and C and D: fibrillation (stretching). Images are 8.5 × 8.5 mm^2. (c) Tack energy on the degreased substrates, with details of contributions. Values are given in J/m^2.

the plasma treatment on the fracture energy of the resins is therefore treated at "iso-max-energy".

3.3.1. Reference Resin. Figure 7a represents the trend for tack curves of the reference on degreased and plasma substrates (Supporting Information Movie S1, Deg—top, Deg—bottom, plasma—top, and plasma—bottom, for the degreased and plasma substrates, respectively) after 140 min of isothermal cross-linking at 120 °C. The curves changed slightly depending on the surface treatment. The cavitation was stronger (points A and B, Figure 7a) on plasma-treated substrates, while both the stretching and flow were weaker (points C and D). Those trends can also be seen in Figure 7b, which shows the snapshot of real-time videos of both tack tests. Stronger cavitation can be seen by a greater number of smaller bubbles (images labeled "point A"). The decrease in flow can be seen by the early sharpening of the bubbles on plasma-treated substrates (images labeled "point B"). The decrease in stretching can be mostly seen toward the end of the test, where fibrils are thinner and longer on degreased substrates (images labeled "D"). From an energy standpoint (Figure 7c), the overall energy dissipated is equivalent on both substrates, supporting the little difference seen in the conversion rate (Figure 3). However, it appears that the plasma treatment increased the cavitation energy by 60%, while decreasing the fibrillation contribution by 30%. Thus, the tack test is sensitive enough to reveal a potential condensation reaction between the amines and the grafted surface ketones not seen by the measurement of the conversion rate (Figure 3). Indeed, this reaction would consume amines, therefore increasing the surface energy (we assimilate it to Dupré's thermodynamic adhesion). On the other hand, more amines consumed on the surface means less amines reacting in the bulk, hence a lower viscoelasticity, translated by a decrease in fibrillation.

3.3.2. M52 Resin. The trend of tack curves for the M52 resin on both surfaces is depicted in Figure 8a (Supporting Information Movie S2, Deg—top, Deg—bottom, plasma—top, and plasma—bottom, for the degreased and plasma substrates, respectively) after 110 min of isothermal cross-linking at 120 °C. The transition from cavitation to flow occurs later on plasma substrates (points A). Bubbles during cavitation are smaller and in greater number (images labeled "A" on Figure 8b), confirming a stronger cavitation. Also, an early stabilization of the pattern is visible in Figure 8b (images labeled "B" and "C"), while the pattern continuously evolved on degreased substrates. For the plasma-treated substrates, a "shrinkage" is clearly observable (images labeled "C"), hinting a strong competition between the viscous flow and the fibrillation. On the associated videos, this shrinkage can be seen to relax, marking the end of the macromolecule orientation (i.e., flow) and the beginning of the macromolecular stretching.

Energywise (Figure 8c), the plasma treatment increased the total energy dissipated from 21 to 55 J/m^2. Moreover, the energy dissipated by cavitation doubled, while the fibrillation energy was multiplied by 4.

https://doi.org/10.1021/acsomega.3c02836
ACS Omega 2023, 8, 37842−37851

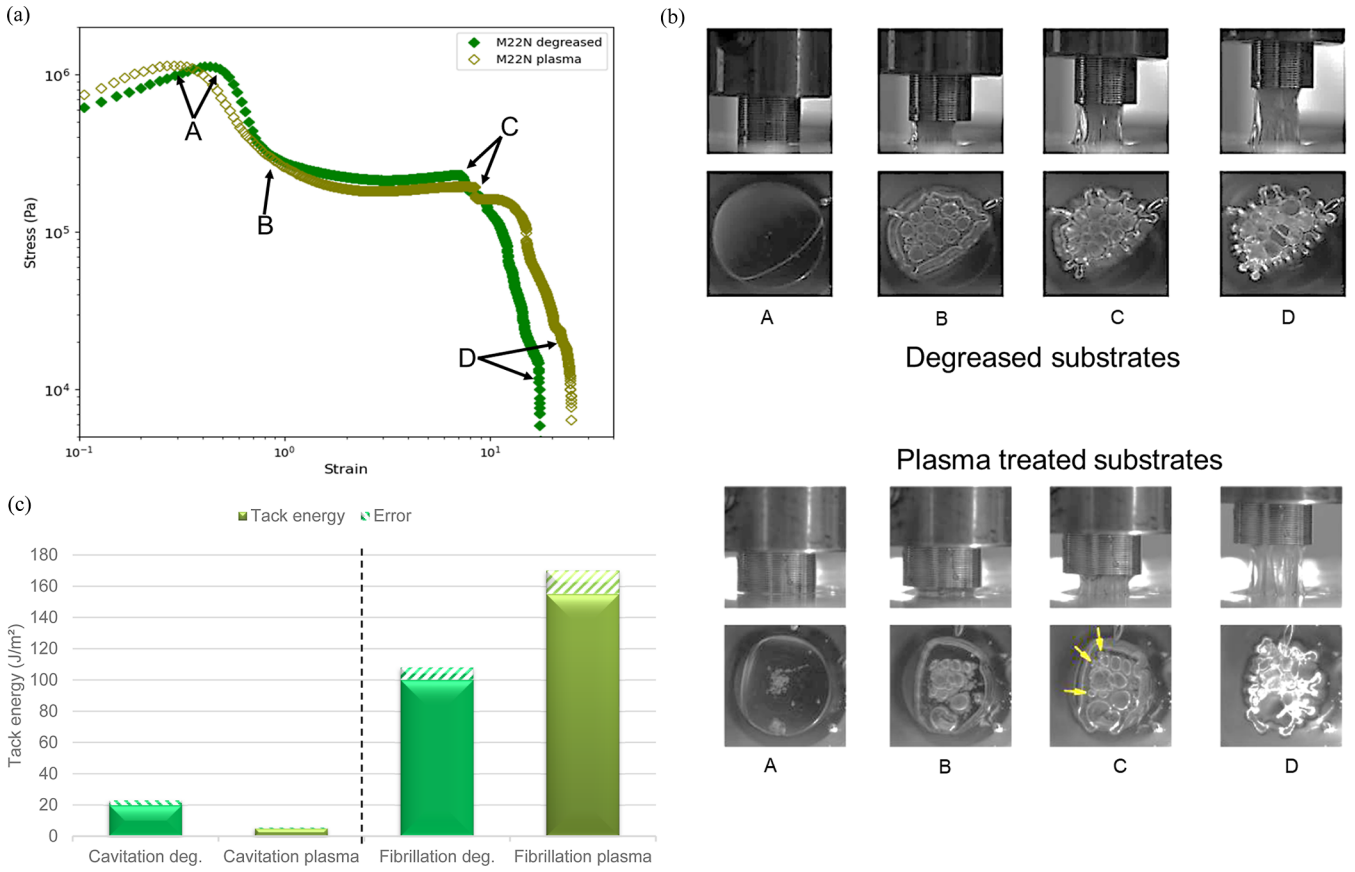

Figure 9. Tack data analysis of the M22N adhesive. (a) Trend of tack curves for the M22N resin, for both degreased (closed symbols) and plasma (open symbols) surface treatments, after an isothermal curing of 130 min at 120 °C. (b) Sampled images from a tack test to illustrate the four zones of Figure 5. A: cavitation; B: fibrillation (flow); and C and D: fibrillation (stretching). Images are 8.5 × 8.5 mm^2. (c) Tack energy on the degreased substrates, with details of contributions. Values are given in J/m^2.

We demonstrated earlier that the plasma treatment reduced the conversion rate. Due to interactions with the surface ketones grafted by the plasma treatment, PMMA's phase separation is less pronounced. Moreover, the grafted ketones may also promote more amine−ketone interactions.

Thus, the increase in cavitation (i.e., surface energy) may be attributed to an increase in surface interactions, namely, amine−ketone and PMMA−ketone. The increase in fibrillation (i.e., bulk energy) may be attributed to the resin being more homogeneous since PMMA is less phase-separated. Thus, PMMA would have a greater reinforcement effect on plasma. This supposition is supported by the fact that the overall energy dissipated is slightly superior when comparing the M52 resin to the reference (21 and 15 J/m^2, respectively), knowing that the conversion rate is inferior (0.42 and 0.51, respectively) (Figure 3). Similarly, PMMA strengthens the cohesion by adding epoxy−PMMA interactions to the balance.

3.3.3. M22N Resin. Yet another scenario occurs for the M22N resin (Figure 9a,b, Supporting Information Movie S3, Deg—top, Deg—bottom, plasma—top, and plasma—bottom, for the degreased and plasma substrates, respectively). After the initial cavitation (points A), competition between flow and cavity expansion prevents any lateral move of the resin (points B). Stretching takes over those two phenomena, which lead to strain-hardening of the resin (points C). On plasma substrates, strain-hardened fibrils provoke a secondary cavitation (Supporting Information S3, plasma—bottom), witnessed by the second plateau after the strain-hardening on the curve.

This resin had a less pronounced cavitation, an increased flow, and an increased stretching on plasma substrates. Cavitation was 4 times weaker than on degreased substrates, but its fibrillation was 50% higher (Figure 9c).

We demonstrated earlier that the plasma treatment increased the conversion rate. Due to PMMA having DMA grafted, the PMMA−ketone interactions led to higher phase separation, disrupting the stoichiometry toward an excess of hardener.

Thus, on plasma substrates, the condensation reaction would be lessened, explaining a decrease in surface energy, and can be seen by a transition cavitation to flow occurring earlier. More amine in the bulk would increase the cohesion (i.e., the solid fraction is higher since the conversion is higher), seen by a prolonged "rubbery" plateau (Figure 9a, portion of the curve between points B and C). Moreover, the M22N resin on plasma can be seen to flow more (Figure 9a, portion of the curve between points A and B), in accordance with a dilution effect of the amines, as shown in Figure 2.

As a brief round-up, we demonstrated that the copolymers overall enhanced the fracture energy measured, increasing both the cavitation and fibrillation contributions regardless of the surface treatment.

On degreased substrates, the M52 resin had both cavitation and fibrillation increased by 1.4, while the M22N resin had its cavitation and fibrillation increased by 4 and 10, respectively.

On plasma-treated substrates, the M52 resin had its cavitation and fibrillation increased by 2 and 6, respectively,

https://doi.org/10.1021/acsomega.3c02836
ACS Omega 2023, 8, 37842−37851

while the M22N resin had its cavitation divided by 4 and its fibrillation increased by 20.

Usually, commercial epoxy resins have a tack energy of about 100 J/m^2. Within this frame, the M22n resin has a tack energy of about 120 and 155 J/m^2, respectively, on degreased and plasma-treated glass. Therefore, the DGEBA + MDEA + M22N resin is a good candidate for use in prepreg made of glass fibers, per "tack energy" standard.

An interesting trend is that resins with a higher conversion rate showed lower cavitation energy and higher fibrillation energy. This may be caused to an extent by the phase separation of the PMMA blocks. Since the conversion rate and phase separation are closely intertwined, we shall not be tempted to discriminate their effects herein. This trend opens attractive follow-up studies in which we may monitor the surface interactions by controlling the grafted reactive functions. Previous interpretations may only be possible thanks to the high sensitivity of the probe tack test. As we have shown herein, the probe tack test is sensitive to assess variations in fracture energy caused by fine changes in both stoichiometric and components' interaction balances.

4. CONCLUSIONS

This study shows that the probe tack test is a sensitive method to evaluate the variations of fracture energy up to gelation, caused by fine stoichiometric variations, a change in the balance of components' interaction, or a combination of both effects, on samples with a relatively low thickness, ca. 300 μm. The probe tack test highlighted a new dissipative phenomenon for thermosetting resins, namely, a viscous flow, only observed for highly viscous liquid. Thermosetting resins have the peculiarity to exhibit cavitation, viscous flow, and fibrillation, all being in competition with each other during a tack test.

Our study also revealed that a change in surface energy, thus in surface functions, has a great impact on the curing behavior before gelation. Above all, we have shown that the tack test is relevant to assessing those changes. Especially, we have been able to measure changes in fracture energy, due to a change of stoichiometry. On the one hand, specific interactions take place due to the peculiar self-association of the copolymers' PMMA block, leading to phase separation, the latter, respectively, accelerating and delaying the curing rates for the M52 and M22N resins. On the other hand, the plasma treatment induced more changes on the PMMA behavior, by inverting the M52 resins' curing rates (rate decreasing compared to untreated samples) and M22N resin (rate increasing compared to untreated samples). Moreover, in the reference, a potential change in the balance interfacial strength (surface energy)—cohesion (bulk energy) due to a shift in the amines' condensation reaction with grafted ketones was easily seen by the tack test, when the measure of the conversion rate was not sensitive enough to that change.

Finally, we showed that the epoxy resins made of DGEBA and MDEA may be suitable candidates for composite application when toughened by M22N copolymers, at least per tack energy standards.

■ ASSOCIATED CONTENT

Supporting Information

The Supporting Information is available free of charge at https://pubs.acs.org/doi/10.1021/acsomega.3c02836.

Top view of a tack test for the reference adhesive on degreased substrates (AVI)

Top view of a tack test for the reference adhesive on plasma-treated substrates (AVI)

Top view of a tack test for the M52 adhesive on degreased substrates (AVI)

Top view of a tack test for the M52 adhesive on plasma-treated substrates (AVI)

Top view of a tack test for the M22N adhesive on degreased substrates (AVI)

Top view of a tack test for the M22N adhesive on plasma-treated substrates (AVI)

Bottom view of a tack test for the reference adhesive on degreased substrates (AVI)

Bottom view of a tack test for the reference adhesive on plasma-treated substrates (AVI)

Bottom view of a tack test for the M52 adhesive on degreased substrates (AVI)

Bottom view of a tack test for the M52 adhesive on plasma-treated substrates (AVI)

Bottom view of a tack test for the M22N adhesive on degreased substrates (AVI)

Bottom view of a tack test for the M22N adhesive on plasma-treated substrates (AVI)

Complex viscosity as a function of the curing time; conversion rate as a function of the curing time and the surface treatment, for the reference adhesive; conversion rate as a function of the curing time and the surface treatment, for the M52 adhesive; conversion rate as a function of the curing time and the surface treatment, for the M22N adhesive; evolution of the tack energy as a function of the cross-linking time at 120 °C; degreased substrates; evolution of the tack energy as a function of the cross-linking time at 120 °C; and plasma-treated substrates (PDF)

■ AUTHOR INFORMATION

Corresponding Author

Valérie Nassiet − *Laboratoire Génie de Production, Ecole Nationale d'Ingénieurs de Tarbes, 65016 Tarbes cedex, France*; Email: valerie.nassiet@enit.fr

Authors

Olivier Tramis − *Laboratoire Génie de Production, Ecole Nationale d'Ingénieurs de Tarbes, 65016 Tarbes cedex, France*; orcid.org/0000-0002-9602-0342

Nicolas Merlinge − *Laboratoire Génie de Production, Ecole Nationale d'Ingénieurs de Tarbes, 65016 Tarbes cedex, France*

Bouchra Hassoune-Rhabbour − *Laboratoire Génie de Production, Ecole Nationale d'Ingénieurs de Tarbes, 65016 Tarbes cedex, France*

Marina Fazzini − *Laboratoire Génie de Production, Ecole Nationale d'Ingénieurs de Tarbes, 65016 Tarbes cedex, France*

Complete contact information is available at: https://pubs.acs.org/10.1021/acsomega.3c02836

Notes

The authors declare no competing financial interest.

https://doi.org/10.1021/acsomega.3c02836
ACS Omega 2023, 8, 37842−37851

■ ACKNOWLEDGMENTS

The authors would like to thank Amandine Abadie for technical support.

■ REFERENCES

(1) Abenojar, J.; Martínez, M.; Encinas, N.; Velasco, F. Modification of Glass Surfaces Adhesion Properties by Atmospheric Pressure Plasma Torch. *Int. J. Adhes. Adhes.* **2013**, *44*, 1−8.
(2) Terpilowski, K.; Rymuszka, D. Surface Properties of Glass Plates Activated by Air, Oxygen, Nitrogen and Argon Plasma. *Glass Phys. Chem.* **2016**, *42* (6), 535−541.
(3) Yamamoto, T.; Okubo, M.; Imai, N.; Mori, Y. Improvement on Hydrophilic and Hydrophobic Properties of Glass Surface Treated by Nonthermal Plasma Induced by Silent Corona Discharge. *Plasma Chem. Plasma Process.* **2004**, *24* (1), 1−12.
(4) Kuliaei, A.; Amiri Amraei, I.; Mousavi, S. R. Investigating the Relationship between Tack and Degree of Conversion in DGEBA-Based Epoxy Resin Cured with Dicyandiamide and Diuron. *J. Polym. Eng.* **2021**, *41* (7), 537−545.
(5) Budelmann, D.; Schmidt, C.; Meiners, D. Prepreg Tack: A Review of Mechanisms, Measurement, and Manufacturing Implication. *Polym. Compos.* **2020**, *41* (9), 3440−3458.
(6) Budelmann, D.; Schmidt, C.; Meiners, D. Tack of Epoxy Resin Films for Aerospace-Grade Prepregs: Influence of Resin Formulation, B-Staging and Toughening. *Polym. Test.* **2022**, *114* (May), 107709.
(7) Tramis, O.; Brethous, R.; Hassoune-Rhabbour, B.; Fazzini, M.; Nassiet, V. Experimental Investigation on the Effect of Nanostructuration on the Adherence Properties of Epoxy Adhesives by a Probe Tack Test. *Int. J. Adhes. Adhes.* **2016**, *67*, 22−30.
(8) Gent, A. N.; Schultz, J. Effect of Wetting Liquids on the Strength of Adhesion of Viscoelastic Material. *J. Adhes.* **1972**, *3* (4), 281−294.
(9) Maiez-Tribut, S.; Pascault, J. P.; Soulé, E. R.; Borrajo, J.; Williams, R. J. J. Nanostructured Epoxies Based on the Self-Assembly of Block Copolymers: A New Miscible Block That Can Be Tailored to Different Epoxy Formulations. *Macromolecules* **2007**, *40* (4), 1268−1273.
(10) Zhou, X.; Johnson, P. F.; Condrate, R.; Guo, Y. Structural investigation of plasma-enhanced glass surface modification using ftir spectroscopy. *Mater. Lett.* **1990**, *9* (5−6), 207−210.
(11) Owens, D. K.; Wendt, R. C. Estimation of the Surface Free Energy of Polymers. *J. Appl. Polym. Sci.* **1969**, *13*, 1741−1747.
(12) Winter, H. H. Can the Gel Point of a Crosslinking Polymer Be Detected by the G'-G\″ Crossover? *Polym. Eng. Sci.* **1987**, *27*, 1698−1702.
(13) Gomez, C. M.; Bucknall, C. B. Blends of Poly(Methyl Methacrylate) with Epoxy Resin and an Aliphatic Amine Hardener. *Polymer* **1993**, *34* (10), 2111−2117.
(14) Zosel, A. Effect of Cross-Linking on Tack and Peel Strength of Polymers. *J. Adhes.* **1991**, *34* (1−4), 201−209.
(15) Chambon, F.; Winter, H. H. Stopping of Crosslinking Reaction in a PDMS Polymer at the Gel Point. *Polym. Bull.* **1985**, *13* (6), 499−503.
(16) Palierne, J. F. Linear Rheology of Viscoelastic Emulsions with Interfacial Tension. *Rheol. Acta* **1990**, *29* (3), 204−214.
(17) Remiro, P. M.; Riccardi, C. C.; Corcuera, M. A.; Mondragon, I. Design of Morphology in PMMA-Modified Epoxy Resins by Control of Curing Conditions. I. Phase Behavior. *J. Appl. Polym. Sci.* **1999**, *74*, 772−780.
(18) Ritzenthaler, S.; Girard-Reydet, E.; Pascault, J. P. Influence of Epoxy Hardener on Miscibility of Blends of Poly(Methyl Methacrylate) and Epoxy Networks. *Polymer* **2000**, *41* (16), 6375−6386.
(19) Galante, M. J.; Oyanguren, P. A.; Andromaque, K.; Frontini, P. M.; Williams, R. J. J. Blends of Epoxy/Anhydride Thermosets with a High-Molar-Mass Poly(Methyl Methacrylate). *Polym. Int.* **1999**, *48* (8), 642−648.
(20) Chen, J.; Taylor, A. Epoxy Modified with Triblock Copolymers: Morphology, Mechanical Properties and Fracture Mechanisms. *J. Mater. Sci.* **2012**, *47* (11), 4546−4560.
(21) Wehlack, C.; Possart, W.; Krüger, J. K.; Müller, U. Epoxy and Polyurethane Networks in Thin Films on Metals - Formation, Structure, Properties. *Soft Mater.* **2007**, *5* (2−3), 87−134.
(22) Possart, W.; Krüger, J. K.; Wehlack, C.; Müller, U.; Petersen, C.; Bactavatchalou, R.; Meiser, A. Formation and Structure of Epoxy Network Interphases at the Contact to Native Metal Surfaces. *C. R. Chim.* **2006**, *9* (1), 60−79.
(23) Creton, C.; Fabre, P. Tack. *Adhesion Science and Engineering*; Elsevier, 2002; Vol. *II*, pp 535−575.
(24) Poivet, S.; Nallet, F.; Gay, C.; Teisseire, J.; Fabre, P. Force Response of a Viscous Liquid in a Probe-Tack Geometry: Fingering versus Cavitation. *Eur. Phys. J. E* **2004**, *15* (2), 97−116.

https://doi.org/10.1021/acsomega.3c02836
ACS Omega 2023, 8, 37842−37851